

Fe and Zn removal from steel making industrial wastewater by electrically enhanced membrane bioreactor

Menatalla A.L. Ahmed, Shadi W. Hasan*

Department of Chemical Engineering, Khalifa University of Science and Technology, Masdar Institute, P.O. Box – 54224, Abu Dhabi, UAE, Tel. +97-128-10 9237, Fax +97-128-10 9901, email: mahmed1@masdar.ac.ae (M.A.L. Ahmed), swajih@masdar.ac.ae (Shadi W. Hasan)

Received 15 March 2017; Accepted 4 August 2017

ABSTRACT

This study aimed at investigating the removal of iron (Fe), zinc (Zn) and bacteria from steel making wastewater. Current density varying between 10 and 20 A/m² was applied. Hydraulic retention time (HRT) and sludge retention time (SRT) of 13.5 h and 10 d were maintained, respectively. Each run was carried out for 45 d. Fe and Zn concentrations in influent wastewater and treated effluent were measured by HACH LCK 321 and LCK 360 vials, respectively. Bacteria content was determined using colony forming unit (CFU). XRF was used to analyze the concentration of Fe and Zn on electrodes deposits and sludge precipitates. Results showed that Fe removal of 98.4 ± 1.1%, 81.1 ± 12.3%, and 38.8 ± 4.2%, and Zn removal of 93.8 ± 2.7%, 71.8 ± 17.7%, and 50.1 ± 17.2 % were reported at 10, 15, and 20 A/m², respectively. Bacteria was reported to have been completely removed by eMBR. Also, XRF analysis at 10 A/m² revealed higher Fe concentration on the electrodes deposits (214.5 ± 8.7 and 3.0 ± 0.1 g/kg on the cathode and anode, respectively) compared to sludge precipitate (48.8 ± 4.9 g/kg). Similarly, XRF analysis at 10 A/m² revealed higher Zn concentration on the electrodes deposits (19.7 ± 3.2 and 0.6 ± 0.3 g/kg on the cathode and anode, respectively) compared to sludge precipitate (8.2 ± 1.8 g/kg).

Keywords: Electrically enhanced membrane bioreactor; Electrodeposition; Electrosettling heavy metals; Industrial wastewater

1. Introduction

Membrane electro-bioreactor (eMBR) is a novel wastewater treatment technology that combines membrane filtration, biodegradation, and electrochemical processes into one system to reduce membrane fouling and enhance effluent's quality [1]. Incorporation of electrochemical treatment introduces electrochemical mechanisms such as electrocoagulation, electroosmosis, and electrophoresis that are responsible for enhancing pollutants removal in addition to controlling the mobility of foulants, and hence their depositions on the membrane surface [1]. The application of electric current releases various metal species in the system as a result of electrodes dissociation; these species are produced

depending on the pH of the media, and contribute to the destabilization and aggregation of suspended solids and colloids through coagulation process [2]. Moreover, electrophoretic motion allows the negatively charged foulants and extracellular polymeric substances to be transported towards the oppositely charged electrodes away from the membrane, and thus reduces the formation of biofilms and membrane fouling [3]. eMBR is a modification on the membrane bioreactor (MBR) widely used technology to enhance effluent quality and reduce membrane fouling [3]. Other fouling control techniques that have been employed when operating MBR are excess aeration and frequent membrane cleaning; however, the application of direct current (DC) has been proven to be the most effective [4]. It was found that applying an intermittent electric field not only requires less power consumption and minimizes the direct exposure of bacteria to the electric field to reduce the negative effects

*Corresponding author.

Presented at the 11th International Conference on Membranes in Drinking and Industrial Water Production (MDIW), 6–8 February 2017, Leeuwarden, The Netherlands

on microbial community, but also has a similar effect on fouling control as the case when continuous electric field is used [5,6].

Previous studies have been conducted on eMBR to investigate the optimum treatment conditions, efficiency of different wastewater purification, and fouling control studies. eMBR has been studied experimentally for the treatment of municipal wastewater [7], industrial wastewater [8], and gray water [9]. Moreover, modeling studies have been performed to explore the performance of the hybrid system when treating different influent wastewater [10]. eMBR has been employed to remove organics (COD), nutrients, color, and turbidity [4]. Most of the conducted studies were performed at a lab-scale. Also, most of the experimental studies were limited to low-to-medium strength wastewater [4].

Industries that generate wastewater rich in heavy metals such as Cd, Cr, Ni, As, and Zn are considered to be the most hazardous due to their high solubility in aquatic environments and potential to be absorbed and bioaccumulated in living cells [11]. Heavy metals can cause serious health effects including reduced growth and development, cancer, and organ damage. For instance, the toxicities associated with high Zn exposure are depression, lethargy, neurological signs and increased thirst. Thus, maximum contaminant level (MCL) value established by USEPA for Zn is 0.8 ppm [11]. Fe, on the other hand, does not have serious health effects but have aesthetic, cosmetic, and technical effects due to its undesirable odor and taste, ability to damage water equipment due to corrosivity, scaling, and sedimentation as well as its potential to reduce effectiveness of treatment for other contaminants. Thus, World Health Organization (WHO) has set the secondary contaminant level for Fe to be 0.3 ppm [12,13]. Table 1 illustrates a summary obtained from literature of some treatment techniques for Fe and Zn removal from wastewater.

To date, no comprehensive experimental study has been performed on wastewater with high heavy metals content, or biologically recalcitrant contaminants. This study

explored the efficiency of eMBR in treating wastewater generated from steel making industry at three different current densities. The reason of choice of steel making industry is its high heavy metals content, particularly Fe and Zn. The removal mechanisms of these metal ions was also discussed thoroughly.

2. Experimental set-up and methods

2.1. eMBR design and current density optimization

Fig. 1 shows an overview of electrically-enhanced membrane bioreactor (eMBR). Different current densities were tested to optimize the removal of Fe and Zn steel making synthetic industrial wastewater. A lab-scale eMBR was tested over three runs with three different current densities, namely, 10, 15, and 20 A/m². The range of current density was selected based on previous studies by the same group of researchers [5,6]. Each current density was studied for a period of 45 d. A constant current density was maintained throughout each experiment by tuning the applied voltage knob. The typical range of applied voltage varied between 5.6–8.5 V, 8.5–12.4 V, and 12.6–15.1 V at 10, 15, and 20 A/m² respectively. The slight increase in the applied voltage is due to the deposition on the surface of the electrodes, which creates resistance and thus increases the required energy supplied.

The total volume of the reactor was 31.5 L, and the effective volume was 22.5 L. The continuous bioreactor was made of polycarbonate walls with a submerged microfiltration (MF) flat sheet membrane supplied by KUBOTA Corporation with a pore size of 0.4 μm. The membrane consists of acrylonitrile butadiene styrene (ABS), polypropylene (PP), polyethylene terephthalate, and chlorinated polyethylene at a proportion of 1:2:2:2. The anodes were made of aluminum sheets with 25% porosity, while the cathodes were thin stainless steel perforated mesh. The electrodes

Table 1

A summary obtained from literature of some methods used for Fe and Zn removal

Method	Comment	Ref.
Electrocoagulation	Current density = 0.06 A/dm ² , 98.8% Fe removal and 95.2% Zn removal.	[14,15]
Ion exchange	Almost 90% Fe removal Effective for water with Fe concentration less than 25 ppm.	[16]
Membrane filtration	Fe removal 80–90%.	[16]
Iron sequestering	Effective for removal soluble Fe The process involves the addition of sequestering agent, such as sodium silicate or polysulphates in conjunction with chlorine.	[17]
Biological removal	Fe removal efficiency 70% Anaerobic condition is more suitable Zn removal by <i>Spirulina platensis</i> .	[16,18] [19]
Adsorption	Adsorption capacity of Zn is: 168 mg/g for powdered waste sludge, 128.8 mg/g for dried marine green macroalgae, 73.2 mg/g for lignin, 55.8 mg/g for cassava waste, and 52.9 mg/g for bentonite.	[20]
Complexation-membrane filtration	The most effective composition for Zn removal is obtained by using: PES-10 membrane, PAA complexation agent at pH > 8.	[21]

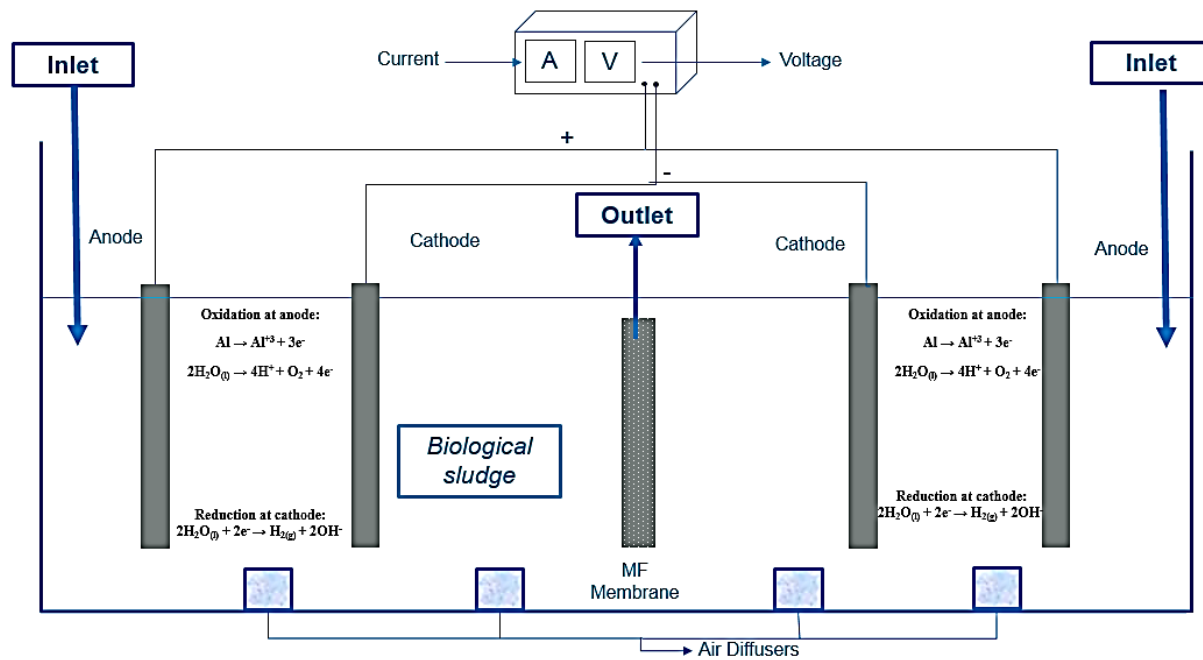


Fig. 1. An overview of an eMBR system.

were designed in a vertical and parallel configuration with a distance of 5 cm between the anode and cathode, and were connected to a direct current power supply with current density varying between 10 and 20 A/m². The anode and cathode were placed at a distance of 5 and 10 cm, respectively, from the membrane, which is located at the center of the reactor. Intermittent current supply of 5 min ON: 15 min OFF was ensured through electronic timer.

There were three zones in the eMBR: the filtration zone, inter-electrode zone, and the anoxic zone. The chosen configuration was A-C-M-C-A (A stands for anode, M stands for membrane, and C stands for cathode). The cathodes were placed adjacent to the membrane at the filtration zone to prevent direct aluminum release from the anode onto the membrane surface. Moreover, this configuration allows coagulated solids to move closer to the electrodes on both sides of the membrane rather than depositing on its surface. Air diffusers were positioned at the bottom of the reactor on both sides of the membrane in the filtration zone in addition to the area between electrodes to scour the membrane, and to maintain aerobic conditions in the inter-electrode zone. The anoxic area is the zone between the anodes and the reactor wall, on both sides. No air bubble diffusers were fixed in the anoxic zone to enhance denitrification.

Membrane cleaning was required when the membrane was clogged, which was indicated by the increase in trans-membrane pressure (TMP) up to ~30 kPa. TMP value was measured using digital pressure gauge (Ashcroft DG25®). Both physical and chemical cleaning were performed. The membrane module was washed with tap water for physical cleaning followed by a 20 h chemical cleaning using 0.06% NaOCl solution.

Synthetic wastewater used in the experiments was prepared in the lab and consisted of (concentrations in mg/L): Glucose (310), Peptone (252), Yeast extract (300), (NH₄)₂SO₄

(200), KH₂PO₄ (37), MgSO₄·7H₂O (40), MnSO₄·H₂O (4.5), FeCl₃·6H₂O (0.4), CaCl₂·2H₂O (4), KCl (25), and NaHCO₃ (25) to simulate the composition of domestic wastewater and add nutrients for microorganisms to function properly [22]. Heavy metals were added to simulate the composition of metals in steel making industry as follows (in mg/L): Fe (24.32), Mn (1.5), Cu (0.09), Pb (0.01), and Zn (4.58) [23]. The wastewater was then fed at a flow rate of 40 L/d by two inflow pumps (in order to pump to both sides of the bioreactor); and one outflow pump discharged clean effluent at a rate of 40 L/d. The sludge inoculums were obtained from a nearby MBR wastewater treatment plant at Masdar city (Abu Dhabi, UAE), with an initial average mixed liquor suspended solids (MLSS) of 2190 ± 278 mg/L. 100 mL of sludge was added to the synthetic wastewater 200 L feed tank every batch to investigate bacterial removal by eMBR.

2.2. Sampling and analytical methods

The performance of the bioreactor was monitored based on the quality of treated effluent. Fresh samples of influent and effluent were collected twice a week and analyzed in duplicates for COD, ortho phosphate (PO₄³⁻-P), Fe, Zn, and ammonia (NH₄⁺-N) using HACH LCK 314, 514, 348, 321, 360, and 303 vials, respectively. HACH DR 3900 bench top Spectrophotometer equipped with radio frequency identification technology was used accordingly. Fe, Zn, COD, PO₄³⁻-P, and NH₄⁺-N removal was measured in terms of percent removal efficiency defined as:

$$\eta(\%) = \frac{C_0 - C}{C_0} \times 100\% \quad (1)$$

where C₀ and C are the concentrations of species in the wastewater influent and treated effluent, respectively.

pH and temperature were measured using DO multi meter (HQ 40d multi model). This study was conducted at room temperature ($21 \pm 2^\circ\text{C}$), pH ranges were 6.7–8.3, 5.2–8.1, and 4.3–7.4 for 10, 15, and 20 A/m^2 , respectively. No chemicals were added to control the pH. Hydraulic retention time (HRT) and sludge retention time (SRT) of 13.5 h and 10 d were maintained. MLSS and mixed liquor volatile suspended solids (MLVSS) were measured according to American Public Health Association (APHA) standard methods, and the measurements involved using MEMMERT UF55 Oven and CARBOLITE CWF 1100 Furnace. The sludge samples were filtered using vacuum filtration by WELCH 2546C-02A vacuum pump. X-ray fluorescence (XRF) analyses were conducted by NITONXL3t 600 XRF analyzer to determine the composition of settled sludge and deposits on electrodes. Organic acid content in the mixed liquor was analyzed using Agilent 1260 High Performance Liquid Chromatography (HPLC) that is composed of binary pump G1312C, degasser G1379B, autosampler G1329B, column thermostat compartment G1316A, Refractive index detector (RI) G1314B, and computer with Agilent Open LAB CDS EZ Chrome software. The column used is Hi-Plex H- column supplied by Agilent, and only the RI detector was used with a wavelength of 250 nm. Bacteria content was determined using colony forming unit (CFU) test which gives a rough estimate of the total counts of viable bacteria (TBC) in a sample before and after the treatment. The agar medium was prepared using Luria Broth recipe; the agar medium components include (all in grams): tryptone (10), yeast extract (5), sodium chloride (5), and agar powder (20) dissolved in 1 L of Millipore Milli-Q® DI water (18.2 $\text{M}\Omega$ cm and 2 ppb TOC at 25°C). The medium was autoclaved at 121°C for 20 min, then poured into plates and left at room temperature to solidify. Interpretation of removal mechanism was provided using Quanta 250 Scanning Electron Microscopy (SEM), Energy Dispersive Spectroscopy (EDS) using NovaNano SEM, and Fourier transform infrared (FTIR) Bruker Vertex 80 v spectroscopy, ATR was used as an accessory and OPUS was used as the interface software.

3. Results and discussion

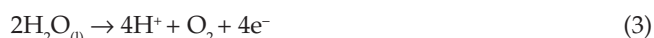
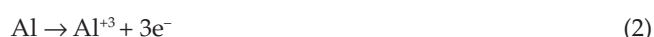
3.1. Removal of Fe and Zn by eMBR

Fe and Zn removal efficiencies were determined for the three current densities. Current density has an effect on the amount of coagulant produced and the rate of gas bubbles generated. As a result, mixing intensity and mass transfer on electrodes are also influenced by current density [24]. Figs. 2 and 3 show that as current density increased, Fe and Zn removal efficiencies decreased. Fe removal was reported to be $98.4 \pm 1.1\%$, $81.1 \pm 12.3\%$, and $36.9 \pm 4.2\%$ for 10, 15, and 20 A/m^2 , respectively. Similarly, Zn removal was reported to be $93.8 \pm 2.7\%$, $71.8 \pm 17.7\%$, and $50.1 \pm 17.2\%$ for 10, 15, and 20 A/m^2 , respectively.

Conversely, most studies conducted have found that increasing the current density is associated with higher removal efficiency of contaminants [25–28], including heavy metals [29–32]. This is attributed to the direct proportionality between current value and potential electrolysis, and thus anodic and cathodic reactions. However,

other studies findings were in agreement with the results obtained from this study [33,34]. In general, these studies found that an increase in current density above its optimum value did not result in an increase in pollutants removal efficiencies as the highest removal was obtained when sufficient numbers of metal hydroxide flocs were available for the sedimentation of the pollutant [35]. The most common mechanism of pollutant removal by electrokinetic treatment is electrocoagulation (EC) in which coagulants are generated physiochemically in the bulk solution in situ by the electrooxidation of sacrificial anodes [36].

The oxidation reaction at anode:



The reduction reaction at cathode:

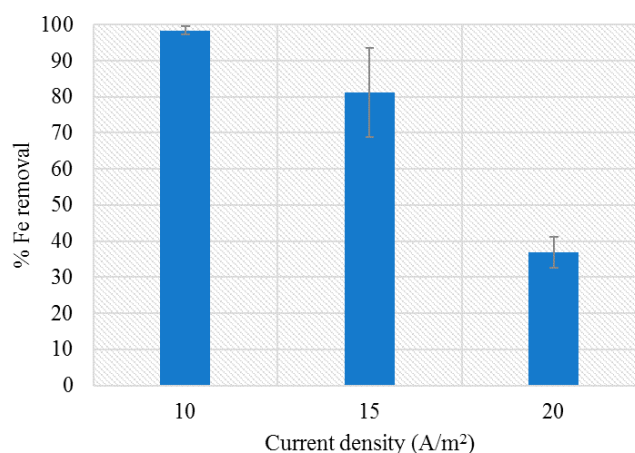


Fig. 2. Average Fe removal vs. current density.

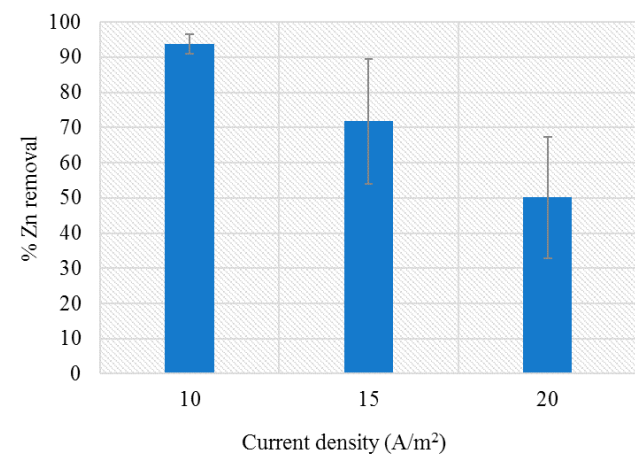


Fig. 3. Average Zn removal vs. current density.

The hydrolysis reaction:



Production of aluminum hydroxides and polyhydroxides such as $\text{Al}_2(\text{OH})_2^{+2}$, $\text{Al}_2(\text{OH})_2^{+4}$, $\text{Al}(\text{OH})_4^-$, $\text{Al}_6(\text{OH})_{15}^{+3}$, $\text{Al}_7(\text{OH})_{17}^{+4}$ and other species take place after the dissolution of the aluminum ions [10], aluminum ions are transformed to aluminum hydroxide at suitable pH values before being polymerized to $\text{Al}_n(\text{OH})_{3n}$ [37]. Cationic $\text{Al}(\text{OH})_2^+$ forms at low pH values, while anionic $\text{Al}(\text{OH})_4^-$ forms at high pH [38]. Moreover, the contaminants are either removed by flotation or sedimentation depending on the amount of current passed. Sedimentation is promoted by low current, while flotation is promoted by high current due to hydrogen gas production [32].

Heavy metals can be removed by sludge by three pathways [39–41]:

- Adsorption: metallic ions are adsorbed on the surface of $\text{Al}(\text{OH})_3$ colloids. The aqueous behavior of aluminum includes the formation of monomeric and polymeric hydroxoaluminum ions such as $\text{Al}(\text{OH})^{+2}$, $\text{Al}(\text{OH})_2^+$, $(\text{Al}_2(\text{OH})_2)^{+4}$, $\text{Al}_6(\text{OH})_{15}^{+3}$, and others [42]. These species polymerize into insoluble amorphous $\text{Al}(\text{OH})_3$. The monomeric and polymeric hydroxoaluminum ions are positively charged complexes that are attracted to negatively charged species and thus are not attracted to heavy metal ions.
- Precipitation of metallic hydroxides. Metal hydroxides, including Fe, are highly insoluble at high pH values [43]. The $\text{Fe}(\text{OH})_{n(s)}$ remains in the aqueous phase as an amorphous suspension, which can further remove other pollutants from the wastewater by either complexation or electrostatic attraction followed by coagulation.
- Heavy metals can be removed biologically by microorganisms using two mechanisms, namely: biosorption and bioaccumulation. Biosorption reactions can be adsorption reactions, ion exchange reactions with functional groups at the cell surface, and surface complexation reactions. Bioaccumulation results in an enrichment of metals ions in the interior of the cell.

The negative correlation between current density and heavy metals removal is attributed to the drop of the mixed liquor medium pH. The pH at which the experiment was operating at current density of 10 A/m² was in the range 8.3–6.7, the pH dropped to 8.1–5.2 when the experiment was running at a current density of 15 A/m² and 7.4–4.3 at 20 A/m². The drop in pH causes H⁺ ions in the solution to be reduced to hydrogen gas at the cathode and the same proportion of hydroxide ions cannot be produced [28], which justifies the further drop in pH. Also, a drop in the pH is associated to heavy metal desorption from colloidal surfaces, which causes adsorbed ions to be leached out into the mixed liquor [39]. Cationic $\text{Al}(\text{OH})_2^+$ is formed at low pH, while anionic $\text{Al}(\text{OH})_4^-$ is formed at high pH. Positively charged heavy metals ions are repelled by the cations, and thus desorption occurs at low pH values [41,44].

The solubility of ferric, ferrous and Zn compounds is highly dependent on the pH in aqueous solutions. The dissolved metal ions in the form of hydrated ions or low molecular weight complexes would pass easily through the MF membranes because of their small sizes compared to the pore size of the membrane [45]. It is important to also know that a very high increase in the pH does not lead to better performance. In general, the solubility of metal hydroxides in solution decreases with increasing pH to a minimum value, namely, the isoelectric point, beyond which metals become more soluble due to their amphoteric nature [46].

A possible speculation for the drop in the removal efficiency is attributed to flotation effect. At low pH values, the increase in hydrogen production causes gas bubbles to attach to the coagulant crystals, which allows them to float on the surface, and hence reduces the contact time between coagulants and pollutants [33,46]. A similar study conducted to investigate the current density's effect on removal efficiency of poultry slaughterhouse wastewater by electrocoagulation reported a similar negative correlation removal efficiency and current density at the pH range 3.0–5.0 [33].

Another reason for the drop in pH in this study can be justified by the production of carbon dioxide as a result of aerobic degradation of organics, which dissolves in water as carbonic acid [47]. Furthermore, lactic acid is released as a by-product of cell metabolism lowering the pH of the media in the dead zones of the bioreactor [48]. The presence of dead zones was clearly observed in the bioreactor while operating at 10 A/m². HPLC was used to quantify organic acid composition in the samples. HPLC results verified the presence of lactic acid at a concentration of 48.0 mg/L, which corresponds to 0.53 mM, in the sample taken at the end of operation time at this current. Samples of the mixed liquor at 15 A/m² and 20 A/m² were analyzed for the presence of organic acids as well, however, organic acid concentrations were below the detection limit of the HPLC machine. Thus, the drop in pH at 15 and 20 A/m² was not caused by organic acids production. As a result, in this study, the production of H⁺ ions as a result of electrochemical and biological reactions outweighs the production of OH⁻ as a result of reduction at cathodes. Also, another speculation, which is related to the chemistry of aqueous solutions, is that when more anionic species are present in a system compared to cationic species, this shifts the equilibrium of water self-ionization towards the production of more H⁺ ions.

3.2. Distribution of Fe and Zn between electrodes deposits and sludge precipitates

3.2.1. XRF analysis of the electrodes deposits

In addition to the adsorption of Fe and Zn ions on aluminum hydroxides flocs and their precipitation as ferric, ferrous, and Zn hydroxides, Fe and Zn are also deposited on electrodes by electromigration [39]. Pollutants and other species migrate and deposit on the oppositely charged electrodes by electrophoresis as a result of the formation of an electric field upon applying DC [3,49]. Consequently, when the pH of the system is within the acidic range, H⁺ ions compete with heavy metal ions and prevent them from getting

adsorbed onto colloids/flocs in mixed liquor [39]. Instead, metal ions migrate to the cathode, oxidize, and are deposited onto the surface. As shown in Fig. 4, XRF analysis for the obtained depositions on electrodes have shown that Fe content on cathodes was 214.5 ± 8.7 , 147.8 ± 7.3 , 21.6 ± 3.1 g/kg for 10, 15, and 20 A/m², respectively, while Fe concentrations on anode depositions were found to be 3.0 ± 0.1 , 34.9 ± 2.5 , and 38.7 ± 4.9 g/kg for 10, 15, and 20 A/m². It can be deduced that Fe was collected predominantly on the cathodes instead of anodes in the case of applying 10 and 15 A/m².

However, for 20 A/m², the amount of Fe collected on the anodes was higher. Depositions on cathodes decreased due to the excess formation of hydrogen gas as pH drops, which allowed electroflotation to take over [33]. The overall removal by electrodes decreased as current density increased, which agreed with the results illustrated in Fig. 2. Similarly, XRF analysis has revealed a similar trend for Zn as shown in Fig. 5. The amount of Zn deposited on the cathodes decreased due to electroflotation, while Zn deposits on the anodes were almost negligible (<0.1 wt%). Zn concentrations on cathodes were found to be 19.7 ± 3.2 , 3.3 ± 1.6 , 2.7 ± 0.1 g/kg for 10, 15, and 20 A/m², while 0.6 ± 0.3 , 0.9 ± 0.2 , and 0.6 ± 0.2 g/kg of Zn were reported to have been deposited on the anodes. Again, these results are in agreement with the results illustrated in Figs. 3 and 6 shows images of collected cathode and anode deposits, it can be clearly seen that the reddish-brown color of cathode deposits verifies the higher presence of Fe in cathode deposits when compared to anode.

3.2.2. XRF analysis of the sludge precipitates

After coagulation, aggregation, and flocculation, the elemental composition of mixed liquor that settled as precipitated sludge due to gravity was analyzed by the XRF analyzer. Fig. 7 illustrates the concentration of Fe present in sludge at the end of operation at the three current densities. XRF analysis showed that Fe concentration in the dried settled sludge (at 105°C for 2 h) was 48.8 ± 4.9 , 39.4 ± 6.8 , and 34.9 ± 3.2 g/kg for 10, 15, and 20 A/m², respectively. Thus, the amount of Fe present in the flocs

decreased as current increased. Similarly, a similar trend was noticed for Zn. XRF analysis revealed that the amount of Zn present in sludge precipitates was 8.2 ± 1.8 , 4.6 ± 2.5 , and 1.8 ± 0.3 g/kg for 10, 15, and 20 A/m², respectively, as shown in Fig. 8. The amount of Zn present in sludge at 15 A/m² is around 50% of that present at 10 A/m², while the amount of Fe settled in precipitates at 15 A/m² is around

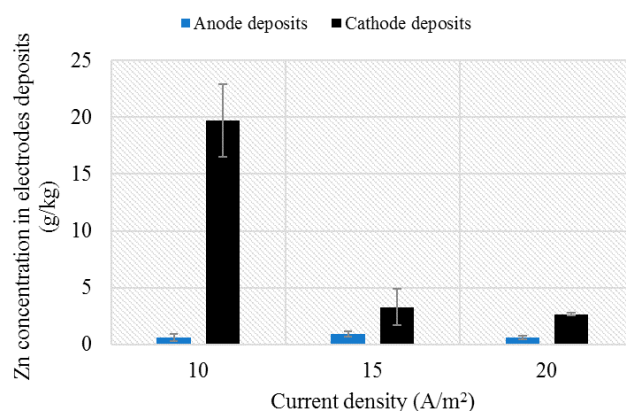


Fig. 5. Zn concentration (g/kg) of electrodes deposits vs. current density.



Fig. 6. Images of collected cathode deposits (LHS) and anode deposits (RHS) at optimum current density (10 A/m²).

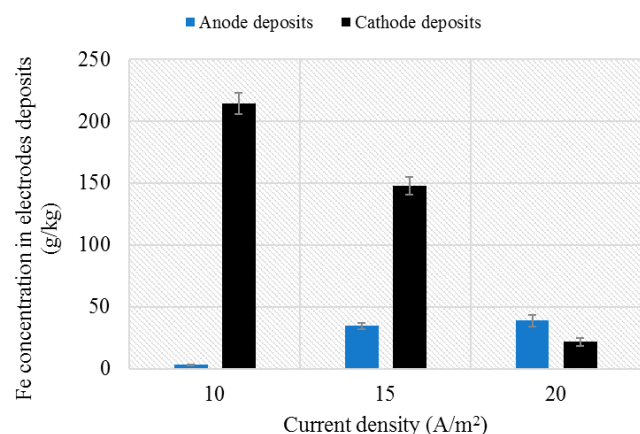


Fig. 4. Fe concentration (g/kg) of electrodes deposits vs. current density.

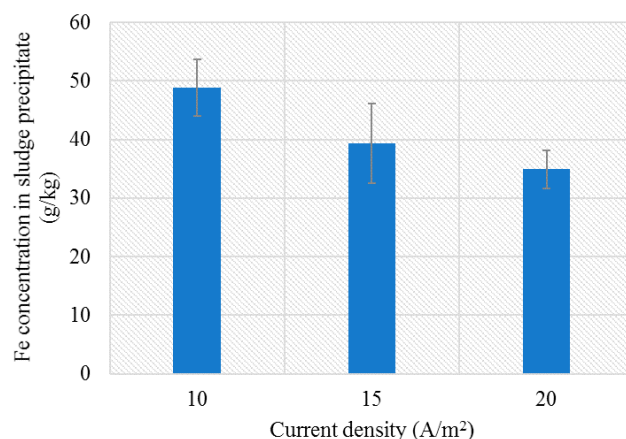


Fig. 7. Fe concentration (g/kg) in sludge precipitate vs. current density.

80% of that settled at 10 A/m². Thus, it can be concluded that Zn is more affected by the drop in pH of the mixed liquor compared to Fe as it was desorbed from the sludge flocs into the solution at a higher magnitude. Furthermore, at optimum current density, results of this study illustrated in Table 2 revealed that the concentration of Zn in sludge is almost 40% of that deposited on electrodes, whereas, the concentration of Fe in the sludge precipitate is only 22.4% of the concentration on electrodes, which reveals that the role of electrosettling is more significant for Zn removal than it is for Fe. Fig. 9 illustrates images of dried sludge precipitate before and after treatment by eMBR at the optimum current density, it can be observed that sludge obtains a reddish-drown color after treatment as a result of the presence of Fe. Fig. 10 shows the changes in flocs morphology after coagulation and metal adsorption.

3.3. General discussion of the XRF analyses of electrodes deposits and sludge precipitates

Comparison of heavy metal concentration in settled sludge precipitates and on electrodes deposits reveals that electromigration is the predominant removal mechanism when compared to electrosettling for both Fe and Zn because the concentration of heavy metals collected on electrodes were higher than those present in sludge precipitates (Table 2). As previously discussed, at optimum current (10 A/m²), Fe was removed more efficiently than Zn by eMBR. This finding was reaffirmed by measuring Fe and Zn concentrations in sludge precipitate as well as electrodes

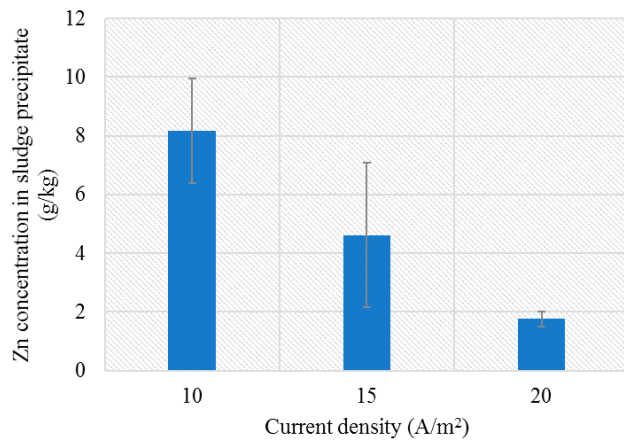


Fig. 8. Zn concentration (g/kg) in sludge precipitate vs. current density.

deposits. Under standard conditions (STP), the experimental hydration enthalpies of Fe⁺² and Zn⁺² were found to be -1950 and -2046 kJ/mole, respectively [50]. Thus, Zn⁺² ions hydrate faster than Fe⁺². This trend is expected because Fe has a larger ionic radii (78 Å) compared to Zn (74 Å), and Zn has a higher charge to surface ratio. The predominant form of Fe ions in aqueous solutions is Fe⁺²(H₂O)₆ hexaquo complex [51], other forms of Fe species that might be present in this study are Fe(OH)₃, Fe(OH)₂⁺, FeOH⁺ according to stability field diagram for aqueous systems that contain ferric and ferrous ions obtained from literature (Eh-pH diagram), which is related to system's pH and voltage applied [52]. Zn ions are present predominantly in the form of Zn⁺²(H₂O)₆, but a more realistic cluster which takes the second hydration sphere into account would be Zn⁺²(H₂O)₁₈ [53]. Therefore, hexahydrated or octadecahydrated Zn ions tend to form complexes with available hydroxyl ions; similarly, hexahydrated Fe ions can exhibit similar behavior. Passing an electric current through the anode causes water electrolysis to take place, thus, oxygen anions are transferred by electrophoretic motion to the anodes, where they are



Fig. 9. Images of dried sludge at the end of operating eMBR at 10 A/m² (LHS) and dried sludge before treatment (RHS).

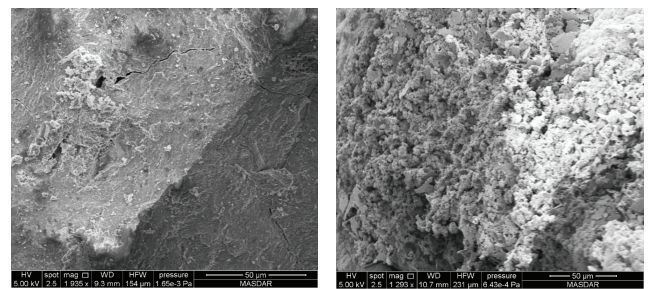


Fig. 10. SEM images of dried sludge before (LHS) and after (RHS) eMBR treatment.

Table 2

A summary of Fe and Zn concentration on cathode deposit, anode deposit, and sludge precipitate

Metal	10 A/m ²			15 A/m ²			20 A/m ²		
	Cathode (g/kg)	Anode (g/kg)	Sludge (g/kg)	Cathode (g/kg)	Anode (g/kg)	Sludge (g/kg)	Cathode (g/kg)	Anode (g/kg)	Sludge (g/kg)
Fe	214.5	2.9	48.8	147.8	35.0	39.4	21.6	38.7	34.9
Zn	19.7	0.6	8.2	3.2	0.9	4.6	2.7	0.6	1.8

oxidized to produce oxygen gas [54]. Similarly, hydrogen gas is released at the cathodes. These gases enhance the horizontal electromigration of positively charged species towards the negative cathodes. This reduces further flocculation and aggregation of dissolved and suspended ionic species in mixed liquor [55]. As previously mentioned, despite the fact that electromigration is the predominant mechanism for both ions removal, the role of electrosettling in Zn removal is more significant. This can be attributed to the second hydration sphere that is formed, which has a higher mass, and thus do not migrate towards the cathodes as easily as Fe complexes do. Another possible reason, is reaction of Zn^{+2} ions with hydrolyzed iron oxides surface hydroxide groups to form metal-complex ($\equiv FeOZn^+$), as will be later verified by FTIR spectroscopy.

3.4. FTIR study of the electrodes deposits and sludge precipitates

The vibrational spectrum of a molecule is considered to be a unique physical property and is characteristic of the molecule. In FTIR spectroscopy, IR radiation is passed through a sample to obtain a unique spectral fingerprint for each molecular structure. As shown in Fig. 11, FTIR spectrum exhibits a broad intense band with a minimum at around 3328 cm^{-1} . This wide band is attributed to the stretching vibration of bonded and nonbonded hydroxyl groups [56]; a broad band at $3600\text{--}3200\text{ cm}^{-1}$ is corresponding to H-bonded OH groups; that is, this broad band is associated with sugar units and alcohols or phenol groups [44–57]. Bands ascribed to proteins and nitrogen containing compounds are located at 1637 and 1539 cm^{-1} . The peak at 1423 is ascribed to carboxylic groups [58], and the band at 1061 cm^{-1} is ascribed to polysaccharide components [59]. Badireddy et al. [60] reported that the peak at ~ 1640

cm^{-1} was associated with the C=O stretching vibration of β -sheets in secondary protein structures, which existed in all EPS samples and favored bio-flocculation [60]. It can be observed that the broadening of this peak takes place due to adsorption of pollutants, which indicates that proteins play a role in the bioadsorption of the pollutants fed into eMBR. The peak corresponding to polysaccharides is located bands between $1200\text{--}1000\text{ cm}^{-1}$ because of their association with the vibrational stretchings of O–H and C–O, the two most common functional groups in any carbohydrate [58].

The peak shift from ~ 1061 to 1036 cm^{-1} indicates a change in substituents on the atoms, which changes the bond strength. The peak at 1418 cm^{-1} , which corresponds to carboxylic groups, appears in both sludge precipitate after operation and electrodes deposits samples, and not in the raw sludge sample. This probably indicates the removal of carbon containing compounds by OH ions. Peaks generated due to weak reflectance in between $1,000\text{--}500\text{ cm}^{-1}$ and $\sim 700\text{ cm}^{-1}$ indicated the presence of miscellaneous oxides and sulfides [61]. The peak at 595 was assigned to Fe–O bonds [62–63]. After the contact with ions in solution, particularly Zn, the peak of Fe–O vibration at around 595 shifted to 442 cm^{-1} . This shift indicates that the direct complexation between Zn cations and Fe compounds might have occurred [64]. Fe oxides were hydrolyzed to surface hydroxide groups that could react with Zn^{+2} ions to form metal-complex ($\equiv FeOZn^+$) as has been reported by Stumm and Morgan for Pb^{+2} ions [65]. The formation of Fe–O–Zn was also reported in other studies using zerovalent iron nanoparticles for Zn removal [66]. Furthermore, the similarity between the peaks in sludge and electrodes deposits samples verifies the action of electromigration of charged species towards the electrodes.

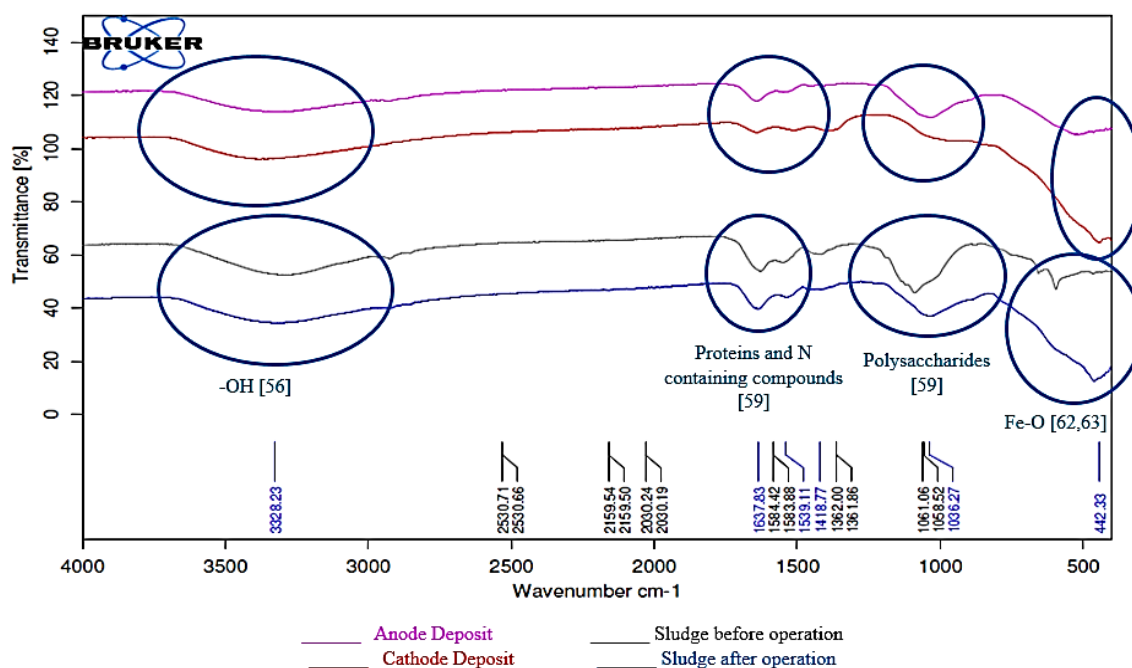


Fig. 11. FTIR analysis of the cathode and anode deposits and dried sludge before and after treatment by eMBR.

3.5. Removal of COD, PO₄³⁻-P, NH₄⁺-N, and bacteria by eMBR

The removal of COD, nutrients and bacteria was also investigated in this study. Figs. 14 and 15 illustrate the removal efficiency of COD and PO₄³⁻-P versus current density. The results show that the removal efficiency of COD and PO₄³⁻-P was slightly affected by increasing current. For example, 89.7 ± 3%, 89.2 ± 3.9%, and 93.1 ± 1.8% COD removal was reported at 10, 15, and 20 A/m², respectively, while PO₄³⁻-P removal was 96.1 ± 3.3%, 99.1 ± 0.5%, 94.3 ± 2.2% at 10, 15, and 20 A/m², respectively. A previous study that investigated the impact of applying current on the same type of biological sludge on bacterial growth rate revealed that bacterial counts reached a maximum at 5 A/m² then decreased significantly at higher current values till it reached 15 A/m², at which the counts remained almost stable; however, the bacterial counts were higher when an electric current was applied when compared to the control case at which no current was applied. The study was conducted at a current density range of 0–20 A/m² at an increment of 5 A/m² [67]. Thus, the aforementioned high removal efficiency of COD and PO₄³⁻-P are resulted from the impact of electric field in the bioreactor. In this study, the increasing MLVSS value at the end of each run when compared to its beginning proves that increasing current within moderate levels did not impede bacterial growth as shown in Table 3. To further understand the reason of COD slight increase with an increasing current, future dynamic studies should be conducted to investigate the behavior of microbial community in an eMBR system and the effect of current density on it.

Some previous studies have found that COD is removed predominantly by biodegradation. Incorporating membrane filtration was found to enhance COD removal, but integrating electrochemical treatment into an MBR system did not have a significant contribution to COD removal [68], while other studies have revealed that eMBR enhances COD removal when compared to the conventional MBR system [8,69]. Thus, COD is removed predominately by biodegradation rather than electrocoagulation. This finding is supported by the elemental analysis of electrodes deposits by SEM/EDS point analysis. Figs. 12 and 13 illustrate the presence of carbon peak, which indicates that electromigration (due to electrokinetic phenomena) has slightly enhanced COD removal. However, as bacterial counts decrease due to increasing current density as previously discussed, electrokinetic reactions cause electrocoagulation to enhance removal, which justifies the increasing COD removal, and the high PO₄³⁻-P removal (94.25%–99.14%).

NH₄⁺-N removal was reported to be 79.2 ± 20.2% at the optimum current density (10 A/m²), 64.1 ± 1.7% and 40.3 ±

4.4% for 15 and 20 A/m², respectively as illustrated in Fig. 16. Nitrifying bacteria are responsible for the conversion of ammonia nitrogen to nitrate nitrogen. The low ammonia removal in this study can be attributed to the direct exposure to DC current. Metabolism of nitrifying bacteria is highly inhibited by electric current due to its effect on the orientation of membrane lipids and thus cell viability [70]. Another reason to decrease ammonia treatment efficiency is the high concentration of heavy metals, particularly Fe, in the synthetic wastewater feed. Iron complexes form a barrier that hinders the transfer of enzymes and nutrients through cell

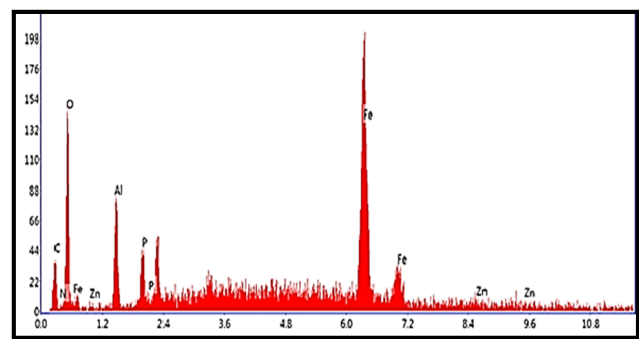


Fig. 12. Elemental analysis of cathode deposits using EDS.

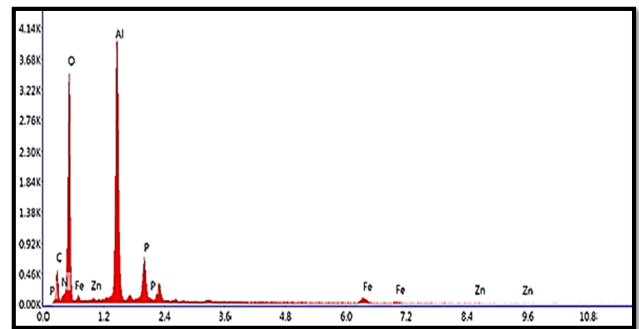


Fig. 13. Elemental analysis of anode deposits using EDS.

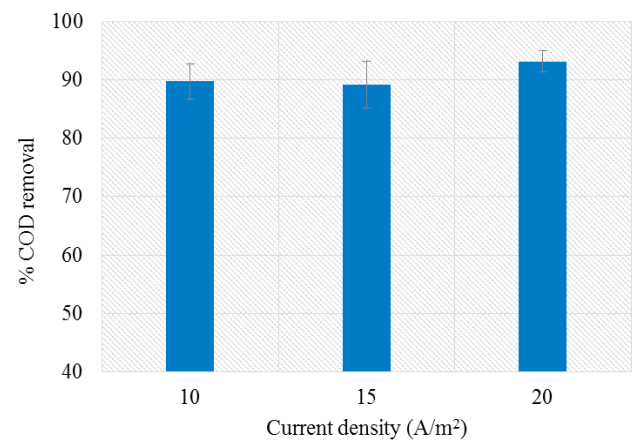


Fig. 14. Average % removal COD vs. current density.

Table 3
MLVSS values at the beginning and at the end of operation period at the three current densities

Current density (A/m ²)	MLVSS at the beginning of operation (mg/L)	MLVSS at the end of operation (mg/L)
10	1682	2213
15	1769	1852
20	1539	1743

membranes [1]. A third reason for the low ammonia removal is due to the accumulation of metal ion complexes produced from electrodisolution of aluminum anodes [4].

Microbiological water quality is usually measured by monitoring the presence of organisms, which are referred to as indicator organisms that might indicate that water is contaminated with fecal pathogens or that disinfection is inadequate. The most highlighted indicator organisms used are

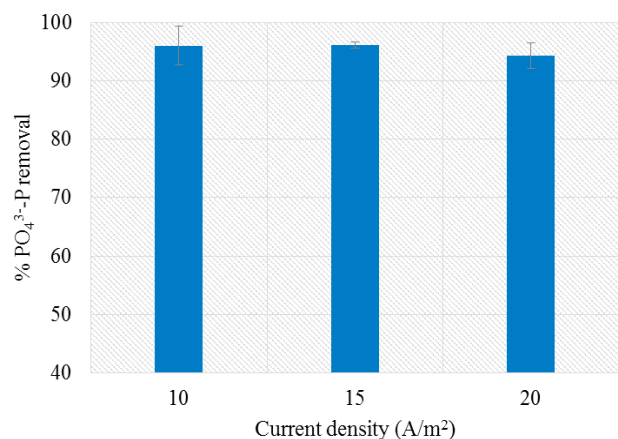


Fig. 15. Average % removal of PO₄³⁻-P vs. current density.

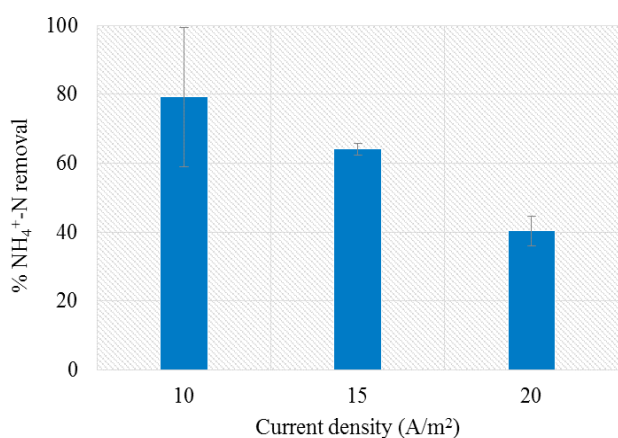


Fig. 16. Average % NH₄⁺-N removal vs. current density.

total coliform (TC) in drinking water quality control, while for wastewater quality control fecal coliform and bacteria *Escherichia coli* are used. Moreover, viruses are considered to be better indicator of water quality than bacteria since they are much smaller and harder to straining than bacteria, and also more resistant to disinfectants [71,72]. For the three current densities, the total bacteria count (TBC) removal by eMBR was 100% when the system was operated at steady state, which corresponds to 0 CFU/100 mL in the effluent. The initial TBC for the influent had an average value of 1,398,000 ± 309218.4 CFU/100 mL. In general, MF membranes have a pore size of 0.1–10 μm. The small pore size of common MF membranes assures the removal of nearly all bacteria from wastewater without the need of any tertiary disinfection to adhere to the regulatory limit [72]. However, if the wastewater fed has a high microbiological content, the membrane shows a poor phage removal. This is expected since the average pore size of the membrane fibers (0.4 μm) which is much larger than the size of the bacteriophage MS-2 (0.02 μm) [73]. It has been suggested that the removal of bacteria as well as viruses is directly linked to the formation of a biofilm on the membrane surface. That is, membrane bioreactor provides three mechanisms for bacteria abatement: a physical factor as a result of reduction based on pore size, a chemical factor attributed to adsorption of bacteria and viruses on the biofilm, and a biological factor resulted from the abatement of phage by other microorganisms present in the mixed liquor [73]. Moreover, electrocoagulation allows further bacteria abatement. A previous study suggests that the main effect of EC on bacterial removal is due to the strong adhesion of bacteria on the surface of electrogenerated alumina due to its nanostructured nature [74]. It is excluded for any electrochemical reaction to take place for bacteria removal by EC due to the presence of phospholipidic membrane to protect bacterial cells. The destruction of these types of membranes requires very strong oxidants [75].

3.6. Membrane fouling evaluation and specific energy consumption of the hybrid system

Membrane fouling rate can be evaluated by measuring the change of TMP in kPa over time of operation; i.e., fouling rate = dTMP/dt. Fig. 18 shows TMP data profile over the entire treatment period. During the 45 d, the fouling rate ranged between 2.3–7.4 kPa/d at the current density that yielded the optimum removal, that is, 10 A/m². Initially

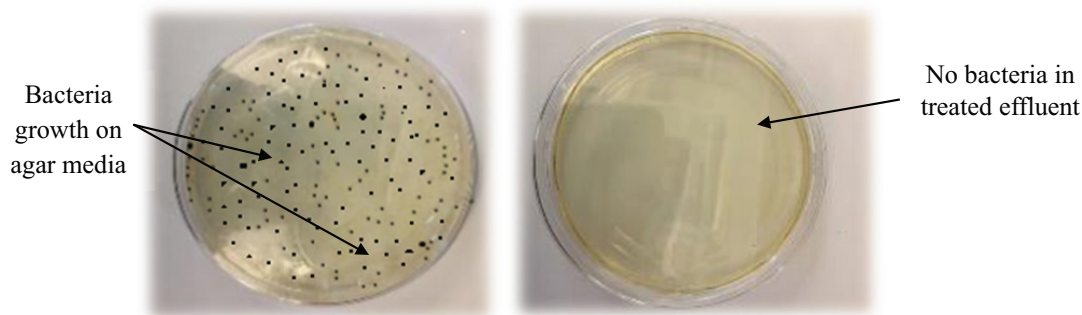


Fig. 17. Total bacteria count (TBC) before (LHS) and after (RHS) eMBR treatment.

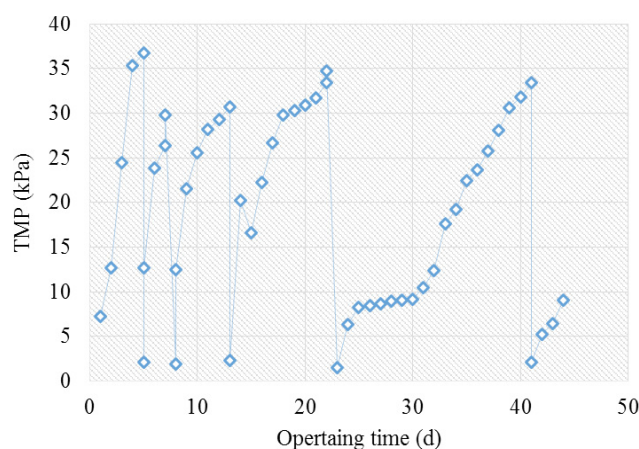


Fig. 18. TMP evolution vs. operating time at 10 A/m².

fouling rate was calculated to be the highest (7.4 kPa/d), then decreased as steady state was reached to be maintained in the range 1.7–3.6 kPa/d. A previous research on eMBR investigated fouling rate at steady state at SRT of 15 days and found that the rate was 6.0 kPa/d. However, the study found that fouling rate was 0.4 kPa/d in the beginning of the run. Clearly, one can conclude that the initial fouling rate in previous work was lower than the one obtained in this study. Conversely, the fouling rate at steady state in this study was lower than the reported previous value. The current density under which the previous study was conducted at was 15 A/m², and the geometry of the electrodes were concentric cylinders as opposed to the parallel plates geometry that was used in this study [76].

The specific energy required by an eMBR is mainly responsible for its operating cost. For this study, applied voltage and current across the reactor configuration were measured. The specific energy consumption was observed to be 1.6–2.5 kWh/m³, 4.0–5.8 kWh/m³, and 8.9–10.7 kWh/m³ for 10, 15, and 20 A/m², respectively. Previous work reported an energy consumption of 6–8 [77] and 4.9–6.1 kWh/m³ [78] for immersed MBR systems. Moreover, previous work on eMBR resulted in specific energy requirements of 0.39–0.87 kWh/m³ [79]. The higher energy consumption is due to the formation of thicker electrodes deposits due to the presence of high concentrations of heavy metals, which leads to higher voltage ranges.

4. Conclusions

Treatment of industrial wastewater, especially those which have a high metal content, has been a major challenge for scholars. A hybrid eMBR technology was tested in this study to evaluate its efficiency in metal ions removal, particularly Fe and Zn. Findings of this study revealed that the highest removal efficiency for both ions was reported when operating at a current density of 10 A/m². It was found that Fe and Zn removal was 98.4% and 93.8%, respectively. Furthermore, electromigration was found to be the predominant mechanism in the removal of both Fe and Zn; electrosettling contributed to the enhanced removal as well. FTIR results revealed a potential mechanism for Zn

removal, which includes the formation of complexes with Fe hydroxides. Also, protein and polysaccharides contribute effectively in the biosorption process. At the optimum current density, 89.7%, 79.2%, and 96.1% removals were reported for COD, NH₄⁺-N, and PO₄³⁻-P, respectively. Moreover, 100% removal of bacteria was reported for the three studied current densities. Therefore, the novel eMBR technology can be applied for industrial wastewater that is rich in heavy metals treatment. Future studies should be conducted in the future to explore the detailed mechanism leading to the complete removal of TBC observed in the effluent of eMBR system. Also, more dynamic studies should focus on investigating the behavior of microbial community in an eMBR system and the effect of current density on its dynamics.

Acknowledgment

The authors gratefully acknowledge Masdar Institute of science and Technology for the financial support (Grant No. SSG2016-000016). KUBOTA Corporation is also appreciated for providing the microfiltration membrane used for this study.

References

- [1] K. Bani-Melhem, M. Elektorowicz, Performance of the submerged membrane electro-bioreactor (SMEBR) with iron electrodes for wastewater treatment and fouling reduction, *J. Memb. Sci.*, 379 (2011) 434–439.
- [2] M.Y.A. Mollah, R. Schennach, J.R. Parga, D.L. Cocke, Electrocoagulation (EC)—science and applications, *J. Hazard. Mater.*, 84 (2001) 29–41.
- [3] J.-P. Chen, C.-Z. Yang, J.-H. Zhou, X.-Y. Wang, Study of the influence of the electric field on membrane flux of a new type of membrane bioreactor, *Chem. Eng. J.*, 128 (2007) 177–180.
- [4] B.M.B. Ensano, L. Borea, V. Naddeo, V. Belgiorno, M.D.G. de Luna, F.C. Ballesteros, Combination of electrochemical processes with membrane bioreactors for wastewater treatment and fouling control: A Review, *Front. Environ. Sci.*, 4 (2016).
- [5] K. Akamatsu, W. Lu, T. Sugawara, S.-i. Nakao, Development of a novel fouling suppression system in membrane bioreactors using an intermittent electric field, *Water Res.*, 44 (2010) 825–830.
- [6] K. Bani-Melhem, M. Elektorowicz, Development of a novel submerged membrane electro-bioreactor (SMEBR): performance for fouling reduction, *Environ. Sci. Tech.*, 44 (2010) 3298–3304.
- [7] S.W. Hasan, M. Elektorowicz, J.A. Oleszkiewicz, Correlations between trans-membrane pressure (TMP) and sludge properties in submerged membrane electro-bioreactor (SMEBR) and conventional membrane bioreactor (MBR), *Bioresour. Technol.*, 120 (2012) 199–205.
- [8] M. Hosseinzadeh, G.N. Bidhendi, A. Torabian, N. Mehrdadi, M. Pourabdullah, A new flat sheet membrane bioreactor hybrid system for advanced treatment of effluent, reverse osmosis pretreatment and fouling mitigation, *Bioresour. Technol.*, 192 (2015) 177–184.
- [9] K. Bani-Melhem, E. Smith, Grey water treatment by a continuous process of an electrocoagulation unit and a submerged membrane bioreactor system, *Chem. Eng. J.*, 198–199 (2012) 201–210.
- [10] A. Giwa, S.W. Hasan, Theoretical investigation of the influence of operating conditions on the treatment performance of an electrically-induced membrane bioreactor, *J. Water Process. Eng.*, 6 (2015) 72–82.
- [11] M.A. Barakat, New trends in removing heavy metals from industrial wastewater, *Arab. J. Chem.*, 4 (2011) 361–377.
- [12] Secondary Drinking Water Standards: Guidance for Nuisance Chemicals, in: U.E.P. Agency Ed., (2013).

- [13] EPA Secondary Maximum Contaminant Levels: A Strategy for Drinking Water Quality and Consumer Acceptability in: P.W.D. Water Research Foundation Ed., (2015).
- [14] S. Vasudevan, J. Jayaraj, J. Lakshmi, G. Sozhan, Removal of iron from drinking water by electrocoagulation: Adsorption and kinetics studies, *Korean J. Chem. Eng.*, 26 (2009) 1058–1064.
- [15] H.J. Mansoorian, A.H. Mahvi, A.J. Jafari, Removal of lead and zinc from battery industry wastewater using electrocoagulation process: Influence of direct and alternating current by using iron and stainless steel rod electrodes, *Sep. Purif. Technol.*, 135 (2014) 165–175.
- [16] S. Chaturvedi, P.N. Dave, Removal of iron for safe drinking water, *Desalination*, 303 (2012) 1–11.
- [17] E.O. Sommerfield, *Iron and Manganese Removal Handbook*, American Water Works Assoc., Denver, US, (1999).
- [18] A.G. Tekerlekopoulou, I.A. Vasiliadou, D.V. Vayenas, Physico-chemical and biological iron removal from potable water, *Biochem. Eng. J.*, 31 (2006) 74–83.
- [19] I. Zinicovscaia, G. Duca, L. Cepoi, T. Chiriac, L. Rudi, T. Mitina, M.V. Frontasyeva, S. Pavlov, S.F. Gundorina, Biotechnology of metal removal from industrial wastewater: zinc case study, *Clean – Soil, Air, Water*, 43 (2015) 112–117.
- [20] H.M. Zwain, M. Vakili, I. Dahlan, Waste material adsorbents for zinc removal from wastewater: a comprehensive review, *Int. J. Chem. Eng.*, (2014).
- [21] G. Borbély, E. Nagy, Removal of zinc and nickel ions by complexation–membrane filtration process from industrial wastewater, *Desalination*, 240 (2009) 218–226.
- [22] M.E.K. Bani-Melhem, J. Oleszkiewicz, Submerged membrane electro-bioreactor (SMEBR) reduces membrane fouling and achieves phosphorous removal, in: WEFTEC, (2009).
- [23] H.A.T.A.A.H. Al-Yazouri, Industrial wastewater treatment using local natural soil in Abu Dhabi, UAE, *Am. J. Environ. Sci.*, 1 (2005) 190–193.
- [24] P.K. Holt, G.W. Barton, C.A. Mitchell, The future for electrocoagulation as a localised water treatment technology, *Chemosphere*, 59 (2005) 355–367.
- [25] Ş. İrdemez, N. Demircioğlu, Y.Ş. Yıldız, Z. Bingül, The effects of current density and phosphate concentration on phosphate removal from wastewater by electrocoagulation using aluminum and iron plate electrodes, *Sep. Purif. Technol.*, 52 (2006) 218–223.
- [26] U. Tezcan Un, A.S. Kopalal, U. Bakir Ogutveren, Fluoride removal from water and wastewater with a batch cylindrical electrode using electrocoagulation, *Chem. Eng. J.*, 223 (2013) 110–115.
- [27] N. Daneshvar, A.R. Khataee, A.R. Amani Ghadim, M.H. Rasoulifard, Decolorization of C.I. Acid Yellow 23 solution by electrocoagulation process: Investigation of operational parameters and evaluation of specific electrical energy consumption (SEEC), *J. Hazard. Mater.*, 148 (2007) 566–572.
- [28] İ.A. Şengil, M. Özacar, The decolorization of C.I. Reactive Black 5 in aqueous solution by electrocoagulation using sacrificial iron electrodes, *J. Hazard. Mater.*, 161 (2009) 1369–1376.
- [29] F. Akbal, S. Camcı, Copper, chromium and nickel removal from metal plating wastewater by electrocoagulation, *Desalination*, 269 (2011) 214–222.
- [30] I. Heidmann, W. Calmano, Removal of Zn(II), Cu(II), Ni(II), Ag(I) and Cr(VI) present in aqueous solutions by aluminum electrocoagulation, *J. Hazard. Mater.*, 152 (2008) 934–941.
- [31] M. Al-Shannag, Z. Al-Qodah, K. Bani-Melhem, M.R. Qtaishat, M. Alkasrawi, Heavy metal ions removal from metal plating wastewater using electrocoagulation: Kinetic study and process performance, *Chem. Eng. J.*, 260 (2015) 749–756.
- [32] D. Ghosh, H. Solanki, M.K. Purkait, Removal of Fe(II) from tap water by electrocoagulation technique, *J. Hazard. Mater.*, 155 (2008) 135–143.
- [33] S. Bayar, Y.Ş. Yıldız, A.E. Yılmaz, Ş. İrdemez, The effect of stirring speed and current density on removal efficiency of poultry slaughterhouse wastewater by electrocoagulation method, *Desalination*, 280 (2011) 103–107.
- [34] I. Ben Hariz, A. Halleb, N. Adhoum, L. Monser, Treatment of petroleum refinery sulfidic spent caustic wastes by electrocoagulation, *Sep. Purif. Technol.*, 107 (2013) 150–157.
- [35] A.A. Bukhari, Investigation of the electro-coagulation treatment process for the removal of total suspended solids and turbidity from municipal wastewater, *Bioresour. Technol.*, 99 (2008) 914–921.
- [36] B. Merzouk, B. Gourich, A. Sekki, K. Madani, M. Chibane, Removal turbidity and separation of heavy metals using electrocoagulation–electroflotation technique: A case study, *J. Hazard. Mater.*, 164 (2009) 215–222.
- [37] M.Y.A. Mollah, P. Morkovsky, J.A.G. Gomes, M. Kesmez, J. Parga, D.L. Cocke, Fundamentals, present and future perspectives of electrocoagulation, *J. Hazard. Mater.*, 114 (2004) 199–210.
- [38] M. Kobya, O.T. Can, M. Bayramoglu, Treatment of textile wastewaters by electrocoagulation using iron and aluminum electrodes, *J. Hazard. Mater.*, 100 (2003) 163–178.
- [39] A. Giwa, I. Ahmed, S.W. Hasan, Enhanced sludge properties and distribution study of sludge components in electrically-enhanced membrane bioreactor, *J. Environ. Manage.*, 159 (2015) 78–85.
- [40] I. Kabdaşlı, I. Arslan-Alaton, T. Ölmez-Hancı, O. Tünay, Electrocoagulation applications for industrial wastewaters: a critical review, *Environ. Technol. Rev.*, 1 (2012) 2–45.
- [41] M. Panizza, A. Barbucci, M. Delucchi, M.P. Carpanese, A. Giuliano, M. Cataldo-Hernández, G. Cerisola, Electro-Fenton degradation of anionic surfactants, *Sep. Purif. Technol.*, 118 (2013) 394.
- [42] P. Cañizares, F. Martínez, C. Jiménez, J. Lobato, M.A. Rodrigo, Comparison of the Aluminum Specification in Chemical and Electrochemical Dosing Processes, *Ind. Eng. Chem. Res.*, 45 (2006) 8749–8756.
- [43] F.M. Tack, O.W.J.J. Callewaert, M.G. Verloo, Metal solubility as a function of pH in a contaminated, dredged sediment affected by oxidation, *Environ. Pollut.*, 91 (1996) 199–208.
- [44] M. Panizza, a. Barbucci, M. Delucchi, M.P. Carpanese, a. Giuliano, M. Cataldo-Hernández, et al., Electro-Fenton degradation of anionic surfactants, *Sep. Purif. Technol.* 118 (2013) 394–398.
- [45] M. Zhao, Y. Xu, C. Zhang, H. Rong, G. Zeng, New trends in removing heavy metals from wastewater, *Appl. Microbiol. Biotechnol.*, 100 (2016) 6509–6518.
- [46] P.K. Holt, G.W. Barton, M. Wark, C.A. Mitchell, A quantitative comparison between chemical dosing and electrocoagulation, *Colloids Surf A Physicochem., Eng Asp.*, 211 (2002) 233–248.
- [47] X.U. Qiyong, G.E. Jiaoju, Reduction of CO₂ emission using bioreactor technology for waste management in China, *Energy Procedia*, 5 (2011) 1026–1031.
- [48] M.A. Hanson, X. Ge, Y. Kostov, K.A. Brorson, A.R. Moreira, G. Rao, Comparisons of optical pH and dissolved oxygen sensors with traditional electrochemical probes during mammalian cell culture, *Biotechnol. Bioeng.*, 97 (2007) 833–841.
- [49] K. Akamatsu, Y. Yoshida, T. Suzaki, Y. Sakai, H. Nagamoto, S.-i. Nakao, Development of a membrane–carbon cloth assembly for submerged membrane bioreactors to apply an intermittent electric field for fouling suppression, *Sep. Purif. Technol.*, 88 (2012) 202–207.
- [50] D.W. Smith, Ionic hydration enthalpies, *J. Chem. Educ.*, 54 (1977) 540.
- [51] E. Kálmán, T. Radnai, G. Pálinkás, F. Hajdu, A. Vértes, Hydration of iron(II) ion in aqueous solutions, *Electrochim. Acta*, 33 (1988) 1223–1228.
- [52] J.D. Hem, Chemical equilibria diagrams for ground-water systems: Les graphiques de l'équilibre chimique pour les systèmes des eaux souterraines, *International Association of Scientific Hydrology*, 5(3) (1960) 45–53.
- [53] W.W. Rudolph, C. C. Pye, Zinc(II) hydration in aqueous solution. A Raman spectroscopic investigation and an ab-initio molecular orbital study, *Phys. Chem. Chem. Phys.*, 1 (1999) 4583–4593.

- [54] S.W. Hasan, M. Elektorowicz, J.A. Oleszkiewicz, Start-up period investigation of pilot-scale submerged membrane electro-bioreactor (SMEBR) treating raw municipal wastewater, *Chemosphere*, 97 (2014) 71–77.
- [55] I.A. Elham Abdulkarem, M. Abu Zahra, S.W. Hasan, Electrokinetic pretreatment of seawater to decrease the Ca^{2+} , Mg^{2+} , SO_4^{2-} and bacteria contents in membrane desalination applications, *Desalination*, 1 (2016).
- [56] G. Haberhauer, B. Rafferty, F. Strebl, M.H. Gerzabek, Comparison of the composition of forest soil litter derived from three different sites at various decompositional stages using FTIR spectroscopy, *Geoderma*, 83 (1998) 331–342.
- [57] F. Nejatizadeh-Barandozi, S.T. Enferadi, FT-IR study of the polysaccharides isolated from the skin juice, gel juice, and flower of *Aloe vera* tissues affected by fertilizer treatment, *Org. Med. Chem. Lett.*, 2 (2012) 33.
- [58] L. Zhu, H.-Y. Qi, M.-l. Lv, Y. Kong, Y.-W. Yu, X.-Y. Xu, Component analysis of extracellular polymeric substances (EPS) during aerobic sludge granulation using FTIR and 3D-EEM technologies, *Bioresour. Technol.*, 124 (2012) 455–459.
- [59] E.J. Martínez, J. Fierro, J.G. Rosas, A. Lobato, M. Otero, X. Gómez, Assessment of cationic dye biosorption onto anaerobic digested sludge: Spectroscopic characterization, *Environ. Prog. Sustain. Energy*, 35 (2016) 1330–1337.
- [60] A.R. Badireddy, S. Chellam, P.L. Gassman, M.H. Engelhard, A.S. Lea, K.M. Rosso, Role of extracellular polymeric substances in bioflocculation of activated sludge microorganisms under glucose-controlled conditions, *Water Res.*, 44 (2010) 4505–4516.
- [61] S.K. Das, A.R. Das, A.K. Guha, Adsorption behavior of mercury on functionalized aspergillus versicolor mycelia: atomic force microscopic study, *Langmuir*, 25 (2009) 360–366.
- [62] A. Akbar, S. Riaz, R. Ashraf, S. Naseem, Magnetic and magnetization properties of iron oxide thin films by microwave assisted sol-gel route, *J. Solgel Sci. Technol.*, 74 (2015) 320–328.
- [63] L. Tang, G.-D. Yang, G.-M. Zeng, Y. Cai, S.-S. Li, Y.-Y. Zhou, Y. Pang, Y.-Y. Liu, Y. Zhang, B. Luna, Synergistic effect of iron doped ordered mesoporous carbon on adsorption-coupled reduction of hexavalent chromium and the relative mechanism study, *Chem. Eng. J.*, 239 (2014) 114–122.
- [64] L. Panda, B. Das, D.S. Rao, Studies on removal of lead ions from aqueous solutions using iron ore slimes as adsorbent, *Korean J. Chem. Eng.*, 28 (2011) 2024.
- [65] W. Stumm, J.J. Morgan, *Aquatic Chemistry: Chemical Equilibria and Rates in Natural Waters*, Wiley, New York, 1996.
- [66] T. Suponik, A. Winiarski, J. Szade, Processes of removing zinc from water using zero-valent iron, *Water Air Soil Pollut.*, 226 (2015) 360.
- [67] M. Zeyoudi, E. Altenaiji, L.Y. Ozer, I. Ahmed, A.F. Yousef, S.W. Hasan, Impact of continuous and intermittent supply of electric field on the function and microbial community of wastewater treatment electro-bioreactors, *Electrochim. Acta*, 181 (2015) 271–279.
- [68] A. Giwa, Modelling and Experimental Investigation of Membrane Bio-Electro-reactor [MBER] for Masdar City Wastewater Treatment, in: *Water and Environmental Engineering*, Masdar Institute of Science and Technology 2014.
- [69] Keerthi, V. Suganthi, M. Mahalakshmi, N. Balasubramanian, Development of hybrid membrane bioreactor for tannery effluent treatment, *Desalination*, 309 (2013) 231–236.
- [70] X.-G. Li, H.-B. Cao, J.-C. Wu, K.-T. Yu, Inhibition of the metabolism of nitrifying bacteria by direct electric current, *Biotechnol. Lett.*, 23 (2001) 705–709.
- [71] N.J. Ashbolt, Microbial Contamination of drinking water and human health from community water systems, *Curr. Environ. Health Rep.*, 2 (2015) 95–106.
- [72] D.S. Francy, E.A. Stelzer, R.N. Bushon, A.M.G. Brady, A.G. Williston, K.R. Riddell, M.A. Borchardt, S.K. Spencer, T.M. Gellner, Comparative effectiveness of membrane bioreactors, conventional secondary treatment, and chlorine and UV disinfection to remove microorganisms from municipal wastewaters, *Water Res.*, 46 (2012) 4164–4178.
- [73] J. Radjenović, M. Matošić, I. Mijatović, D. Barceló, *Membrane Bioreactor (MBR) as an Advanced Wastewater Treatment Technology*, Springer Berlin Heidelberg, Berlin, Heidelberg, 2008, pp. 37–101.
- [74] C. Ricordel, C. Miramon, D. Hadjiev, A. Darchen, Investigations of the mechanism and efficiency of bacteria abatement during electrocoagulation using aluminum electrode, *Desal. Water Treat.*, 52 (2014) 5380–5389.
- [75] M. Li, J.H. Qu, Y.Z. Peng, Sterilization of *Escherichia coli* cells by the application of pulsed magnetic field, *J. Environ. Sci.*, 16 (2004) 348–352.
- [76] S. Ibeid, M. Elektorowicz, J.A. Oleszkiewicz, Novel electrokinetic approach reduces membrane fouling, *Water Res.*, 47 (2013) 6358–6366.
- [77] S. Zhang, R. van Houten, D.H. Eikelboom, H. Doddema, Z. Jiang, Y. Fan, J. Wang, Sewage treatment by a low energy membrane bioreactor, *Bioresour. Technol.*, 90 (2003) 185–192.
- [78] J.A. Gil, L. Túa, A. Rueda, B. Montaña, M. Rodríguez, D. Prats, Monitoring and analysis of the energy cost of an MBR, *Desalination*, 250 (2010) 997–1001.
- [79] S.W.H.A. Giwa, Statistical correlation analysis and energy consumption of electrically-enhanced membrane bioreactor for wastewater treatment, *Desal. Water Treat.*, 68 (2017) 60–69.